

## Experimental investigation of spillback nozzle performance via pulsating LED shadowgraphy

Giovanni Cafaggi\*<sup>1</sup>, Peter Arendt Jensen<sup>1</sup>, Peter Glarborg<sup>1</sup>, Kim Dam-Johansen<sup>1</sup>

<sup>1</sup>Technical University of Denmark, Department of Chemical and Biochemical Engineering, Søtofts Plads, 2800-Kgs.Lyngby, Denmark

\*Corresponding author: [gioc@kt.dtu.dk](mailto:gioc@kt.dtu.dk)

### Abstract

In this study, the atomization characteristics of a commercial spillback hydraulic nozzle were investigated in terms of droplet size and velocity distributions. The spray was produced with a cold setup that can replicate the operating conditions of a commercial auxiliary marine boiler. The measurements were performed using a pulsating LED optical imaging system that employs a CCD camera to capture pairs of frames with a delay as short as 1 $\mu$ s from one another. Positions, velocity, sizes and shapes of single droplet were obtained by analysing the images. Mixtures of water and glycerol were used as model fluids to reproduce a range of physical properties comparable to those found by rheology studies for fuels used in this application. In addition to obtaining the droplet size and velocity distribution for the spray currently used in boilers, the general performance of the nozzle was examined in a series of experiments by varying three parameters: pressure drop, flow rate through the nozzle and liquid viscosity. Results include droplet size and velocity distributions in different spray regions, and a description of the influence of each varying parameter on global indexes such as the SMD.

### Keywords

Experimental, Shadowgraphy, Spillback Nozzle, Characterization

### Introduction

This study is part of a research project on auxiliary marine boilers, where spillback nozzles are employed to atomize liquid fuels prior to evaporation and combustion [1]. The droplet sizes and velocity are of primary importance for flame stability, shape and position, which in turn affect emissions and efficiency of the boiler [2]. Indeed, further insight into spray characteristics at different operating condition could improve the understanding of the boiler behaviour. Moreover, when modelling a full-scale system with finite volume methods, the spatial discretization needed to observe the atomization process is much smaller than the other characteristics lengths. As an approximation, already atomized droplets can be injected in the computational domain, thus avoiding modelling directly the atomization process, but to do so detailed data regarding droplet sizes and velocities are needed.

Spray characterization has been carried out for a commercial pressure swirl spill return nozzle, for three different supply pressures, volume flow rates through the nozzle orifice and liquid viscosities. The position, size, velocity and trajectory direction of more than 600,000 single droplets have been obtained and stored in a database, divided by each operating condition. These data are then also used to conduct a quantitative analysis of the effect of variations of each parameter on spray characteristics.

### Material and methods

In order to investigate the atomization process, an experimental setup was built at DTU. The setup is composed of two systems: one is the hydraulic and safety devices to reproduce at room temperature the spray generated in the full-scale boiler (Figure 1), the second is the shadowgraphy system to capture the spray and measure the droplet properties (Figure 2). The nozzle used in this study is a commercial spillback hydraulic nozzle, rated for a supply pressure of 20 bar and a maximum flow rate of 125 l/h. The nozzle orifice has a diameter of 1mm. This is the same nozzle mounted in the full-scale auxiliary marine boiler, where the nozzle is used to atomize different types of fuels including marine diesel and Heavy Fuel Oil (HFO). There the flow through the nozzle is changed to satisfy a variable steam demand. The nozzle is most commonly used for a flow rates between 50 and 112 l/h. Therefore, it was decided to operate the setup at the extremes of this range, and to include an intermediate value of 80 l/h. Another parameter that can be easily changed in boiler operation is the supply pressure to the nozzle. This is set by the operator and does not require any change to the system for a broad range. Since this parameter is of fundamental importance for atomization quality in pressure swirl atomizer [3], the setup has been built with components able to withstand a wide range of pressures and the nozzle have been tested at three supply pressures: 15, 20 and 25 bars. Higher pressures can be reached by just replacing the safety valve spring and the pressure gauges, as the other components are rated for pressures up to 100 bar. Lastly, the effect of changes in viscosity was explored by

using water-glycerol solutions with viscosities of 5 and 15 cP in the setup [4]. This was done to reproduce the viscosities of the fuels used in the boiler [5].

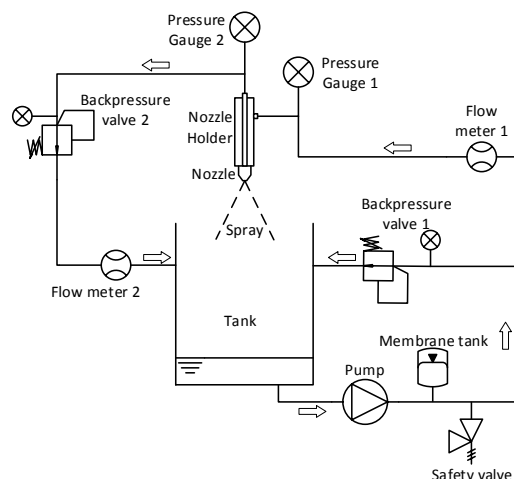


**Figure 1:** Hydraulic system of the spray characterization setup.

The setup is operated with the two backpressure valves, which are used to keep the respective upstream pressure constant, thus regulating supply and spill pressure for the nozzle. A volumetric pump with multiple pistons is used to deliver flow rate in excess of the required amount and part of it is spilled through the first backpressure valve. A membrane tank is used to further reduce any pulsation in the flow. Pressure gauges has been placed as close as possible in the system to the nozzle to monitor supply and spill pressure. The atomized liquid and all the liquid spills are collected into a cylindrical tank and recirculated into the system. To avoid droplet recirculation to the near nozzle region, a raised lid with a hole with the diameter of the boiler burner tube is used and air is sucked by a shielded ventilation connection at the bottom of the tank. The influence of these precautions on the results should be negligible, considering that the spray measurements are taken few centimetres below the nozzle orifice and that the distance to the ventilation and air escape route is approximately one meter. Moreover, it can be argued that this configuration is more similar to that of the full-scale boiler than a closed tank or a completely open environment. The shadowgraphy setup main components are a CCD camera and an LED pulser, synchronized by a delay generator. This type of system has been described elsewhere [7] and the configuration used in this work has been thoroughly tested in previous publications [6], with the only difference being that the telecentric lens used has been replaced with one with a magnification of 1.5x. The camera's CCD sensor is composed of  $1296 \times 966$  pixels and has a total size of  $4.86 \times 3.62$  mm, with a depth of field of 0.86 mm the observed volume is  $6.72 \text{ mm}^3$ . Using the delay generator to flash the LED pulser, pairs of images are taken with a  $5 \mu\text{s}$  delay from one another with a frequency of 20 fps. From the images obtained, each contiguous dark region is measured if its greyscale value are below a certain threshold and its boundary gradient above another. The delay between the frames is set small enough that the distance each droplet moves between frames is small compared to the distance between droplets, thus each droplet in the first frame is paired with the closest one to its position in the second frame. Since we are interested in single droplets and not gas flow velocity as in classical PIV, the velocity vector of each individual droplet is estimated by measuring the distance of the centre in two consecutive snapshots and dividing it by the

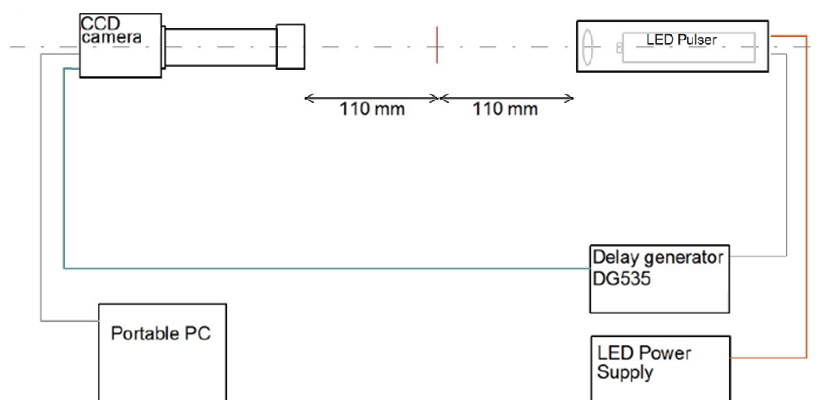


**Figure 2:** Shadowgraphy image acquisition system diagram [6].

delay set between the two frames. Regardless of how sparse the droplet are, it is always possible that some are very close to each other, or that a droplet leaves the sampling volume, and thus different droplets are paired together. To avoid this, it is checked that there is no significant changes in droplet shape, sharpness and droplet size between the paired droplets and that the resulting droplet velocity is within reasonable limits. Also, any potential droplet that cannot be matched in the second frame or that has a diameter of less than three pixels is filtered out, since it is not possible to determine its velocity or shape respectively. This produces the floor value of the droplet diameters, which is clearly visible Fig.3, left. The precision of the droplet diameter estimation is determined by several factors. The first is the error on the pixel size, which is calculated with an optical target, and it is subject to an error below 1%. Secondly, there is an error due to the fact that pixels are not infinitesimally small, this leads to an uncertainty on the position of the boundary of each droplet. This error is reduced by processing the images in greyscale, thus also pixels partly obscured are taken into consideration. While it is difficult to give a precise estimate of the latter factor, the overall accuracy has been tested in previous work [6] with calibration microspheres. These particles belonged to three different diameter intervals corresponding approximately to 5, 10 and 40 pixels. The measured mean diameter for each of the three groups were within the certified particles size range, which spanned respectively 6.2%, 2.8% and 1.7% of the mean. Therefore, the overall relative measurement error is smaller than these percentages, with the highest uncertainty on the smaller droplets and the lowest on the larger ones. To observe different regions of the spray, the system is mounted on a railing system so that the axial and radial distances of the observed volume from the nozzle orifice can be adjusted independently. For this study, all measurements have been taken from 32 to 35 mm downstream of the nozzle orifice and the radial position has been changed in 2.5 mm steps, thus covering the whole spray cross-section. The number of droplets captured in each frame varies with the position and the spray that is being observed: on the outer fringe of the spray most images are empty, while in the central region more than 50 droplets per image are measured. For each experiment, around 400 image pairs have been recorded at each position. The measurements have been stopped when less than 100 droplets were recorded on such samples. It should of course be noted that this is an arbitrary limit and that statistical significance of the findings is lower in the more dilute regions of the spray.

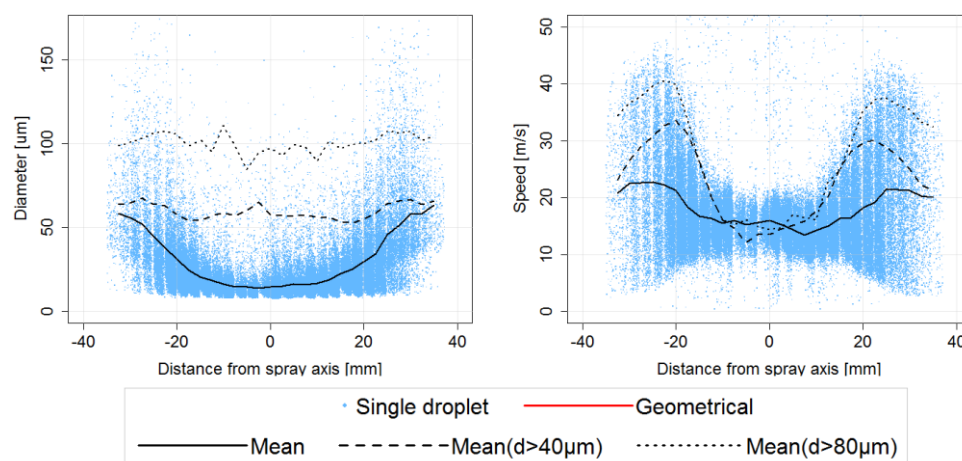


**Figure 3:** Droplet diameter (left) and speed (right) across the spray.

## Results and discussion

Two types of results have been obtained: detailed information about the change in droplet size and velocity across the spray, and effects of changes in operating condition on the spray. While local measurements have been taken for all experiments, for the sake of simplicity the plots reported are for operation with water at 20 bar of supply pressure and a flow rate of 80 l/h, and the average values are referred to the image set taken in each position. The plots report both single droplet values, and average values for each sampling position. The average values are given both for the entire population, and droplets above the the 90<sup>th</sup> and 98<sup>th</sup> quantiles in terms of droplet size to help visualize different trends dependent on particle size.

As also reported in other studies [8], it was observed that the droplet size increases farther away from the spray axis (on the left in Figure 3), while this is expected, it should also be noted that the change is mainly due to the concentration of small droplets toward the “hollow” core of the spray. It can be observed in Figure 3 (left) that when considering only the droplets with a size above the 90<sup>th</sup> percentile, the average size is constant across the spray. The droplet average velocity is lower close to the spray axis (Figure 3, right). In this region average velocity of the droplets is similar, regardless of droplet size, with almost no droplet slower than half of the average value. When moving away from the axis, larger droplets move significantly faster than smaller ones and a significant fraction of droplet assumes velocities interior to those found in the hollow core.

To fully define the droplet movement, it is also necessary to consider the direction of the trajectory of each droplet. This can be quantified as the angle it forms with the spray axis when assuming that the radial component is negligible. The rarity of droplets that move out of focus, compared to that of droplets moving out of the pictures in the image sets support the validity of this assumption, but further validation is required. As a reference, the geometrical angle has been calculated as the angle between the spray axis and the line connecting the nozzle orifice to the sampling position. This would then be the angle of all particles if they moved in a straight line from the orifice. It is interesting to see that the largest droplets seem to move exactly like this (Figure 4). When considering all droplets instead the average angle has an absolute value consistently smaller than the geometric one, and at the centre of the spray a complex behaviour. This effect is probably related to the local gas flow field, since smaller droplets tend to follow it more closely than larger ones.

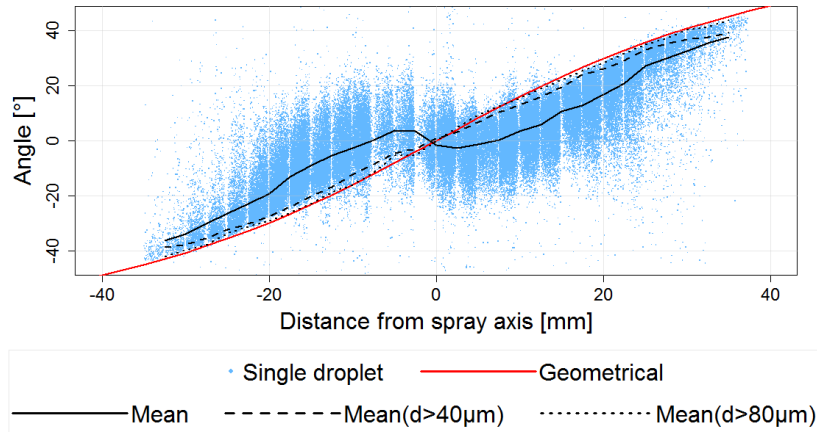


**Figure 4:** Angle of droplet trajectory with the spray axis across the spray.

The results for changes in supply pressure have been obtained by regulating the spill pressure to maintain the atomized flow constant. Another series of experiments instead was done by maintaining the supply pressure constant and adjusting the spill pressure to obtain three different liquid flow rates through the orifice. In this way, it was possible to observe the contribution of varying supply pressure and flow rate separately.

Spill-return atomizer are especially thought to deliver a constant atomization quality on a wide range of flows, and in fact when looking at the overall droplet size it is observed that to large changes in the flow rate, correspond to almost negligible changes in the SMD ( $D_{32}$ ) with no definite trends.

On the other hand, changes in supply pressure have a clear effect on the droplet size: as one would expect, higher supply pressure does indeed produce finer droplets. To use the same nomenclature found in literature, pressure difference is used instead of the supply pressure. In these experiments they are interchangeable because the environment pressure was constant. It was also possible to compare the data with experimental correlations found in literature for pressure swirl nozzles, by calculating the exponent  $\gamma$  as:

$$D_{32} \propto \Delta P^\gamma \quad (1)$$

$$\gamma = \log_{(\Delta P_1/\Delta P_2)}(D_{32,1}/D_{32,2}) \quad (2)$$

This can be done because in these experiments nozzle geometry, flow rate through the orifice and liquid properties are unchanged. In these circumstances, several classical experimental correlations for SMD in pressure swirl nozzles [9][10][11][12] can be simplified and written in the same form as equation 1. A value for  $\gamma$  of  $-0.46 \pm 0.05$  was obtained from the data, matching quite well the values reported in the cited literature, which are all in the range from -0.4 to -0.55.

The same procedure can be applied to the SMD found by changing viscosity of the liquid using water-glycerol solutions. This is done by replacing the pressure difference in equations 1 and 2 with the dynamic viscosity of the liquid. The values obtained for  $\gamma$  in this case is  $0.13 \pm 0.03$ , while values between 0.16 and 0.25 are given in the references. This discrepancy could be attributed to the decrease in surface tension of the liquid when increasing the amount of glycerol in the mixture.

**Table 1:** SMD, average droplet velocity and cone angle for the experimental campaign.

$\Delta P$ [bar]	V [l/h]	$\nu$ [cP]	SMD [ $\mu\text{m}$ ]	$u_{\text{avg}}$ [m/s]	$\beta$ [°]
20	80	1	57.4	32.1	77
15	80	1	66.4	30.0	72
25	80	1	52.5	33.9	77
20	50	1	53.3	31.0	91

20	112	1	54.1	37.9	66
20	112	5	69.6	39.3	60
20	112	15	77.8	37.6	55

The effect of changing flow rate and supply pressure on average droplet velocity and cone angle have been investigated. The average droplet velocity shows that an increase in either parameter, results in an increase droplet speed (Table 1). While this result was expected, it was also interesting to observe that for the same relative change, an increase in flow rate produces an effect three times bigger than a change in supply pressure. Viscosity does not seem to affect droplet speed significantly. The spray cone angle was measured as the angle of the measurement in each set with the highest liquid fraction and it is therefore on a discrete scale. From Table 1, it is possible to see how the spray cone angle decreases at higher viscosities and flow rates through the nozzle, while the change in supply pressure has a negligible effect on it (as reported also by [8][13]).

## Conclusions

The spray generated with a spill return nozzle has been studied using the LED pulsed shadowgraphy technique. Three supply pressures, three liquid viscosities and three different flow rates were investigated during the experiments, thus lending some insight into the effect of each of these parameters. The relation between SMD and changes in supply pressure and viscosity was described with a proportionality exponent  $\gamma$ . The results were compared to those found in literature, showing a good match for supply pressure and a partial one for viscosity. Changes in atomized flow, showed little impact on the SMD. Consistent trends were also found between spray cone angle and both flow rate and viscosity, and lastly between droplet mean velocity, flow rate and supply pressure. The droplet size, velocity and trajectory across the spray were discussed and general trends established for different droplet size fractions. Overall, a sizable dataset to use in boiler modelling was gathered, and a good understanding of the effects on atomization characteristics caused by changes in boiler operation was achieved.

## Nomenclature

$d$	single droplet diameter [ $\mu\text{m}$ ]
$\text{SMD}, D_{32}$	Sauter Mean Diameter [ $\mu\text{m}$ ]
$u_{\text{avg}}$	mean droplet velocity [m/s]
$V$	volume flow rate through the nozzle orifice [l/h]
$\beta$	angle with the spray axis [ $^\circ$ ]
$\gamma$	proportionality exponent [-]
$\Delta P$	pressure difference between supply and environment [bar]
$\nu$	dynamic viscosity [cP]

## References

- [1] G. Cafaggi, P. A. Jensen, P. Glarborg, and S. Clausen, "CFD simulations on marine burner flames," in *Nordic Flame Days*, 2017, pp. 1–6.
- [2] P. Jenny, D. Roekaerts, and N. Beishuizen, "Modeling of turbulent dilute spray combustion," *Progress in Energy and Combustion Science*. 2012.
- [3] A. H. Lefebvre, *Atomization and Sprays*. Hemisphere, 1988.
- [4] N. Cheng, "Formula for the Viscosity of a Glycerol-Water Mixture," *Ind. Eng. Chem. Res.*, vol. 9, no. 47, pp. 3285–3288, 2008.
- [5] L. Zhou, A. Shao, H. Wei, and X. Chen, "Sensitivity analysis of heavy fuel oil spray and combustion under low-speed marine engine-like conditions," *Energies*, vol. 10, no. 8, 2017.
- [6] F. Cernuschi *et al.*, "Accurate particle speed prediction by improved particle speed measurement and 3-dimensional particle size and shape characterization technique," *Powder Technol.*, vol. 318, pp. 95–109, 2017.
- [7] J. Estevadeordal and L. Goss, "PIV with LED: Particle Shadow Velocimetry (PSV) Technique," in *43rd AIAA Aerospace Sciences Meeting and Exhibit*, 2012, no. January 2005.
- [8] J. Jedelsky and M. Jicha, "Energy considerations in spraying process of a spill-return pressure-swirl atomizer," *Appl. Energy*, vol. 132, pp. 485–495, 2014.
- [9] A. H. Lefebvre, *Gas Turbine Combustion*. WASHINGTON, D.C.: Hemisphere, 1983.
- [10] A. K. Jasuja, "Atomization of Crude and Residual Fuel Oils," *ASME J. Eng. Gas Turbines Power*, vol. 101, no. 2, pp. 250–258, 1979.
- [11] A. Radcliffe, "Fuel Injection," in *High speed Aerodynamics and Jet Propulsion*, Princeton, N.J.: Princeton University Press, 1960.
- [12] K. R. Babu, M. V. Narasimhan, and K. Narayanaswamy, "Prediction of Mean Drop Size of Fuel Sprays from Swirl Spray Atomizers," in *2nd International Conference on Liquid Atomization and Sprays*, 1982, pp. 99–106.
- [13] B. Mandal, P. Barman, A. Kushari, and P. Associate, "Study of Primary Atomization in a Helical Passage Pressure-Swirl," in *Proceedings of 19th ILASS Europe*, 2004.